Journal of Crystal Growth 311 (2009) 1487–1492

Contents lists available at ScienceDirect

Journal of Crystal Growth

journal homepage: www.elsevier.com/locate/jcrysgro

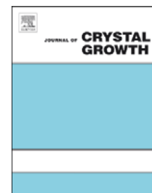

The effect of AlN buffer growth parameters on the defect structure of GaN grown on sapphire by plasma-assisted molecular beam epitaxy

Yuen-Yee Wong [a], Edward Yi Chang [a,*], Tsung-Hsi Yang [b,d], Jet-Rung Chang [b], Yi-Cheng Chen [b], Jui-Tai Ku [c], Ching-Ting Lee [e], Chun-Wei Chang [f]

[a] *Department of Material Science and Engineering, National Chiao Tung University, Hsinchu 30010, Taiwan*
[b] *Department of Electronics Engineering, National Chiao Tung University, Hsinchu, Taiwan*
[c] *Department of Electrophysics, National Chiao Tung University, Hsinchu, Taiwan*
[d] *Microelectronics and Information System Research Center, National Chiao Tung University, Hsinchu, Taiwan*
[e] *Institute of Microelectronics, National Cheng Kung University, Tainan 70101, Taiwan*
[f] *Taiwan Semiconductor Manufacturing Company, 8, Li-Hsin Rd. 6, Hsinchu Science Park, Hsinchu 30077, Taiwan*

A R T I C L E I N F O

Article history:
Received 30 May 2008
Received in revised form
10 November 2008
Accepted 29 December 2008
Communicated by E. Calleja
Available online 6 January 2009

PACS:
61.10.−i
61.71.Hh
81.05.Ea
81.15.Hi

Keywords:
A1. Defects
A1. High-resolution X-ray diffraction
A3. Molecular beam epitaxy
B1. Gallium nitride

A B S T R A C T

The defect structure of GaN film grown on sapphire by plasma-assisted molecular beam epitaxy (PAMBE) depends on the growth temperature and thickness of the aluminum nitride (AlN) buffer layer. High-resolution X-ray diffraction was used to measure symmetric (0 0 0 2) and asymmetric $(1 0 \bar{1} 2)$ rocking curve (ω-scans) broadening, which allowed the estimation of screw threading dislocation (TD) and edge TD densities, respectively. For GaN grown on lower-temperature buffer, the density of screw TD was increased while the density of edge TD was decreased. Further examinations revealed that the edge TD was closely related to stress in GaN film and the screw TD was controlled by AlN surface roughness. Since the GaN defect was dominated by edge TD, the total TD was also effectively suppressed with the use of lower-temperature buffer with appropriate thickness.

© 2009 Elsevier B.V. All rights reserved.

1. Introduction

Molecular beam epitaxy (MBE) has proven to be a promising technique to grow GaN materials for high electron mobility transistor (HEMT) devices fabrication [1–3]. The advantages of growing GaN with MBE include real-time monitoring of crystal growth with reflection high-energy electron deflection (RHEED), a carbon- and hydrogen-free growth environment, a smooth surface, sharp interfaces and low point defect density. These attributes are important for achieving high-quality materials for HEMT devices. However, due to the lack of large native substrate, most GaN materials are grown on a foreign substrate such as sapphire or silicon carbide. In order to compensate the large mismatches in both crystal lattice and thermal expansion coefficient, a suitable buffer layer (such as low-temperature GaN or AlN) is needed for the growth of GaN film on these substrates. For GaN grown using MBE, an AlN buffer is always used to achieve the Ga-face material [4,5], which is needed to obtain the proper polarity to induce two-dimensional electron gas (2DEG) at the AlGaN/GaN interface for high-quality HEMT applications.

Despite the use of buffer layers, GaN grown on these substrates is associated with high dislocation density ($>10^{10}\,cm^{-2}$). Dislocations generated in GaN are mainly screw, edge and mixed TDs. Many researches have been carried out to study the characteristics of these defects. The most commonly used methods to characterize TDs in GaN are X-ray deflection (XRD) [6,7], transmission electron microscope (TEM) [8–10] and atomic force microscopy (AFM) [11,12]. On the other hand, efforts to reduce the high density of dislocation in GaN are also a continuous endeavor of many researchers toward a better quality GaN material. Methods that have been studied include the use of different types of buffer materials (AlN, GaN) or their variations [13–15], the

*Corresponding author. Tel.: +886 3 5131536; fax: +886 3 5724727.
E-mail addresses: edc@mail.nctu.edu.tw, yuenyee98@yahoo.com (E.Y. Chang).

0022-0248/$ - see front matter © 2009 Elsevier B.V. All rights reserved.
doi:10.1016/j.jcrysgro.2008.12.051

insertion of AlN interlayers [3] or Si delta-doping layer [7] and the growth of GaN epilayers on a lateral epitaxial overgrown substrate [16] or a vicinal sapphire substrate [17].

Although intensive studies were carried out on the characterization and reduction of dislocation in GaN, little is known about the relationship between the different kinds of defect structures. In this paper, we have investigated the dependence of different kinds of dislocations on the AlN buffer growth parameters. We also found that the understanding of their relationship can be used to reduce the total dislocation density in GaN.

2. Experiment procedures

The epitaxial layer of GaN and AlN were grown by rf-MBE (ULVAC MBE System) on sapphire (0 0 0 1) substrates. The epi-ready substrates were first thermally cleaned in the MBE chamber at 820 °C for about an hour until the RHEED pattern became streaky. Nitridation of the substrates was then performed at 600 °C to form a starting layer for the deposition of AlN buffer layers, which were grown under different conditions. To investigate the dependence of the GaN defect structure on these AlN buffers, a 2-μm GaN film was deposited with constant growth parameters. Prior to this study, the growth parameters of the GaN film were initially optimized using the homoepitaxial growth approach. The homoepitaxial growth was carried out by depositing the film on a high-quality GaN film (2 μm thick) grown on sapphire by metal-organic chemical vapor deposition (MOCVD) (referred here as the GaN-template). This approach proved useful for growing high-quality GaN film by MBE [18,19]. The optimized growth temperature of the GaN was 740 °C with an effective Ga/N ratio slightly higher than unity (Ga-droplet about to form on GaN surface [8]). To determine the influence of the AlN buffer properties on GaN quality, buffer layers were deposited at different growth temperatures (from 450 to 840 °C) and thicknesses (from 4 to 30 nm). In the first part of these experiments, AlN with constant thickness of 15 nm was used. These samples were labeled as shown in Table 1. In situ RHEED was used to monitor the growth of the AlN and GaN films. RHEED patterns on all the GaN films grown in our experiment were streaky indicating a flat surface (will be determined later) during growth and showing 2 × 2 surface reconstruction upon cooling (indicating a Ga-face polarity [20]) as shown in Fig. 1. On the other hand, the RHEEDs for AlN were somewhat less streaky indicating that their surfaces were less smooth as a result of lower than unity Al/N ratio being used [21]. This ratio was chosen to avoid the formation of Al droplets on the AlN and cubic face GaN at the hetero-interface which could deteriorate the GaN quality [9,21].

Table 1
FWHM of GaN (0 0 0 2) and (1 0 $\bar{1}$ 2) planes grown on different AlN buffer growth temperatures.

Sample	A	B	C	D	E	F
AlN buffer growth temperature (°C)	450	485	525	740	800	840
FWHM of (0 0 0 2) plane (arcsec)	797	636	252	180	79	65
FWHM of (1 0 $\bar{1}$ 2) plane (arcsec)	1385	1870	1526	2323	2331	2400

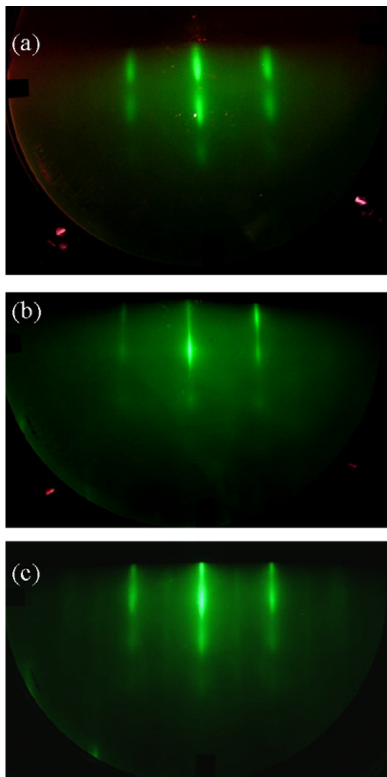

Fig. 1. Typical RHEED patterns for the (a) AlN buffer, (b) GaN film during growth and (c) GaN film after cooling.

3. Results and discussion

Defect structures of the GaN films were determined by high-resolution X-ray diffraction (HRXRD, Bede D1 system). Using double-axis configuration, the rocking curves (ω-scans) for both the symmetric plane (0 0 0 2) and asymmetric plane (1 0 $\bar{1}$ 2) were scanned for each sample. There are three types of threading dislocations in GaN: screw TD (with Burger vector $b=\langle 0001 \rangle$), edge TD ($b=\frac{1}{3}\langle 1\bar{1}20 \rangle$) and mixed TD ($b=\frac{1}{3}\langle 1\bar{1}23 \rangle$). The screw dislocation can distort all the ($h\,k\,i\,l$) planes with l non-zero, while the edge TD can distort only the ($h\,k\,i\,l$) planes with either h or k non-zero. Therefore, the (0 0 0 2) rocking curve is broadened by the screw- or mixed-type TDs while the (1 0 $\bar{1}$ 2) rocking curve is broadened by all TDs [13,22]. If a suitable method is used to estimate the contribution of edge TDs in the broadening of (1 0 $\bar{1}$ 2) rocking curve, measurement of these rocking curve widths can be used to calculate the dislocation densities of both screw and edge TDs in GaN films. Full-width at half-maximum (FWHM) of the rocking curves was determined by non-linear least-squares fitting to a pseudo-Voight function. Table 1 summarises the rocking curve widths of GaN (0 0 0 2) and (1 0 $\bar{1}$ 2) planes grown on different growth temperature AlN buffers. As shown, the (1 0 $\bar{1}$ 2) FWHM was reduced with the increase of (0 0 0 2) FWHM. Or in other words, the reduction of the total dislocation density in GaN film was associated with an increase of screw or mixed TDs when lower-temperature AlN buffers were used.

In order to estimate the dislocation densities in GaN film, the following equation can be used [23]:

$$D_{dis} \sim \beta^2 / 9b^2 \quad (1)$$

where D_{dis} is the TD density in the film, β is the FHWM value of a given XRD peak and b is the length of Burgers vector of the corresponding dislocation. To simplify the calculation of dislocation densities, the mixed TD was divided into edge- and screw-type TDs [13]. So the ‘edge TD’ used in this study was the sum of pure edge-type and the edge component of the mixed-type, while the ‘screw TD’ was the sum of pure screw-type and the screw component of the mixed-type. Then, the rocking curve width

caused by the edge TD in the GaN films can be estimated from the $(10\bar{1}2)$ scan using the following equation:

$$\beta^2_{(10\bar{1}2)} = \beta^2_s + \beta^2_e \quad (2)$$

where $\beta_{(10\bar{1}2)}$ is the FWHM of $(10\bar{1}2)$ plane, and β_s and β_e, are the contributions of screw and edge TDs to the FWHM of $(10\bar{1}2)$ planes, respectively [13]. Using Eqs. (1) and (2), the screw and edge TD densities of GaN can be calculated and the results are plotted in Fig. 2. This figure clearly shows that the edge TD density in GaN film was reduced with the increase of screw TD density. In general, GaN films grown on lower-temperature buffer have a lower edge TD density and higher screw TD density, than GaN films grown on higher-temperature buffer. Even though the edge TD is dominated in all cases, consistent with previous studies of MBE-grown GaN [9,22], it can be effectively suppressed with the use of a buffer layer grown at lower temperature. The edge TD density reduced from 1.5×10^{10} to $3.3\times10^{9}\,cm^{-2}$ when temperature was decreased from 840 to 450 °C. Since the edge TD densities were at least an order of magnitude larger than that of the screw TD (except sample F), the total TD density was also reduced in the similar trend (from 1.5×10^{10} to $3.9\times10^{9}\,cm^{-2}$) despite a significant increase of the screw TD density in the film. On the other hand, the generation of screw TD was restricted by using higher-temperature buffer layers. Screw TD density as low as $4.1\times10^{6}\,cm^{-2}$ was achieved for GaN film grown on the 840 °C AlN buffer.

Further study was carried out to investigate the correlation between defect structure in GaN films and growth temperature of AlN buffer. It is well known that the residual stress can cause the formation of dislocation in a material. Thus, the stress in GaN is also believed to have played a role to manipulate the defect structure in it. The stress in our GaN film was determined by measuring the strain in the GaN lattice constants. Because the GaN epilayer grown on sapphire exhibits in-plane isotropic elastic properties, its in-plane stress (σ) can be described by the lattice strain (ε) from the relationship σ=$M\varepsilon$, where M is the biaxial elastic modulus of GaN. In order to accurately calculate the stress in GaN film grown on sapphire, however, more comprehensive XRD surveys on various asymmetric planes are needed [24]. In this paper, the stress states in GaN films were represented by the deformation of its c-axis lattice constants (ε_c). When the hexagonal GaN film is biaxially stressed on sapphire, its in-plane lattice deformation (ε_a) is associated with out-of-plane lattice change as described by the relationship $\varepsilon_c \propto -\varepsilon_a$. Thus, the stress states in the GaN can be illustrated from the deformation of its c-axis lattice constant. Using triple-axis configuration from the same X-ray diffractometer, the deflection angles of (0002) plane were obtained with high accuracy (within a few arcsec) to determine the c-axis lattice constant of GaN films grown on different temperature AlN buffers. Fig. 3 shows that the edge TD density was increased proportionally with the strain in the GaN film. All the films were compressively stressed with their c-axis lattice constants elongated to different degrees. Increment of the edge TD density from 3.3×10^{9} to $1.5\times10^{10}\,cm^{-2}$ corresponded to the elongation of the c-axis lattice constant from 0.15% to 0.38%. Therefore, the result reveals that the stress in the GaN film has a significant influence on the edge TD as well as the total defect density. For comparison, the data for GaN film grown on the Ga-template (total thickness of about 3 μm) is also shown in Fig. 3. The edge TD density of this sample was only $2.5\times10^{8}\,cm^{-2}$, with the c-axis lattice constant elongated to merely 0.09%. This means that the GaN grown on the GaN-template has the least inherent stress and, thus, the best crystal quality.

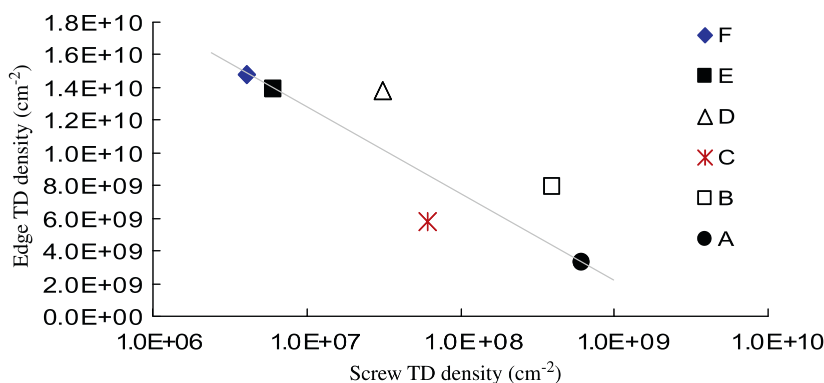

Fig. 2. The screw and edge TDs densities of GaN grown on different temperature AlN buffer layers.

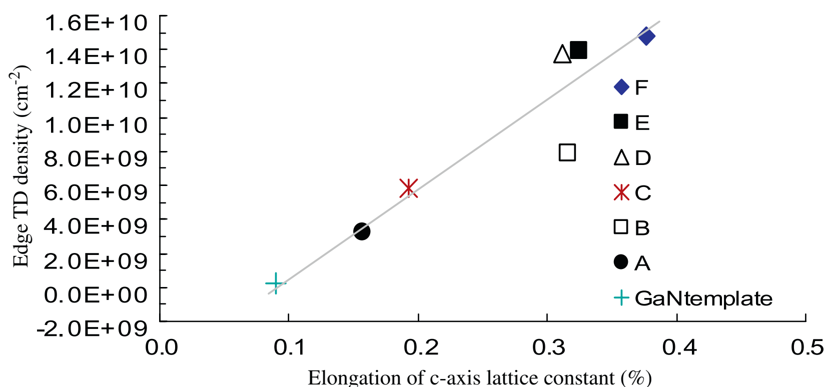

Fig. 3. The dependence of edge TD density on the elongation of c-axis lattice constant for GaN grown on AlN buffer layers prepared at different temperatures.

From the result shown in Fig. 2, it appears that the screw and edge TD densities were controlled by the properties of AlN buffers. To clarify this, we have carried out another set of experiments to grow only the AlN buffer layers on sapphire without GaN films on them. The growth procedure was identical to that described before. After the AlN buffers with nominal thickness of 15 nm were deposited at temperatures shown in Table 1, substrate temperatures were briefly increased/decreased to the growth temperature of GaN before they were cooled to room temperature. The crystal property and the surface morphology of these AlN buffers were characterized using XRD and AFM, respectively. Here, due to weak signals from the thin AlN layers, only rocking curve of its symmetrical (0 0 0 2) plane was scanned. It was surprising to find that the width of (0 0 0 2) rocking curves of all the samples were almost the same, varied between 119 and 128 arcsec, without a clear changing trend against their growth temperature. The small variation in rocking curve widths has suggested that the crystal quality of AlN was not affected by the different growth temperatures used in this study. However, results from the AFM scans have shown that the surface roughness of AlN layers was decreased gradually when the growth temperature was increased in the experiment. In Fig. 4, three representative AFM images show that the surface roughnesses (rms) of AlN grown at 450, 740 and 840 °C were 0.42, 0.29 and 0.19 nm, respectively. For AlN grown at lower temperature, the shorter diffusion length of Al atoms was seemed to create more nucleation sites on sapphire when they reacted with the nitrogen radicals. The AFM images also show that the density of these "nuclei" was larger on a lower-temperature AlN surface. These results, thus, imply that the distribution of different defect structures in the GaN was influenced by the surface roughness of AlN buffer layer. Higher screw TD density was generated in the GaN film when grown on the rougher AlN buffer surface. This is agreed with the finding of Shen et al. [25], who have suggested that the small nuclei on AlN buffer were the origin of spiral growth features that further developed into screw TD in the GaN film. On the other hand, the edge TD density was reduced with the AlN surface roughness. This phenomenon will be discussed later.

In view of the different roughnesses in AlN buffers deposited at different temperatures, we have also investigated the surface morphology of GaN films grown on them. SEM images (Fig. 5) show that the surfaces of GaN films were flat for samples C to F (with AlN buffer temperatures increased from 525 to 840 °C, only image of sample C was shown in Fig. 5(a)). The surface roughness (rms) of sample C (roughest among the samples C to F) was 0.56 nm on a $1 \times 1\ \mu m^2$ area. However, for GaN films grown on AlN buffers lower than 525 °C, some hexagonal shape features appeared on the GaN surfaces as shown in Fig. 5(b) and (c) for samples B and A, respectively. These features could most probably be related to the screw or mixed type TDs which are always grown following a spiral course into a surface hillock with hexagonal boundary [6,8]. Some of these features were quite large (3–4 μm) and with hexagonal-like polygon boundaries, especially for those on sample A. This might be caused by the clustering of many screw/mixed TDs grown in the close vicinity. Therefore, it is believed that these features were the consequences of rough AlN surface grown below 525 °C and high screw/mixed TD ($>10^8\ cm^{-2}$) in the GaN film.

In this study, we were particularly interested in the formation origin of edge TD, which is dominant in GaN grown by MBE and more deleterious to the material electrical properties. As seen before, the edge TD was closely related to the stress in GaN film which was controlled by the growth temperature of AlN. Now, we would also like to see the effect of AlN thickness on the edge TD in GaN films. AlN grown at 525 °C with relatively lower edge TD density and smooth surface has been chosen to further investigate the influence of buffer thickness on the edge TD density. GaN grown on AlN deposited at 525 °C but with different thicknesses (from 4 to 30 nm) was prepared. The changes of both GaN edge TD density and lattice strain on AlN thickness was illustrated in Fig. 6. As shown, the lowest strain and lowest edge TD density were achieved on a 15-nm-thick AlN buffer. This value is comparable to those reported by other groups (~20 nm) for optimized GaN quality [2,3]. Besides, the screw TD densities were about the same for all these samples ($\sim 6 \times 10^7\ cm^{-2}$, not shown here). For GaN grown on sapphire by MBE, AlN is always used to achieve Ga-face GaN. Although AlN has a lattice constant intermediate between film and substrate, it is physically harder and thermally more stable than the GaN buffer which is normally used in

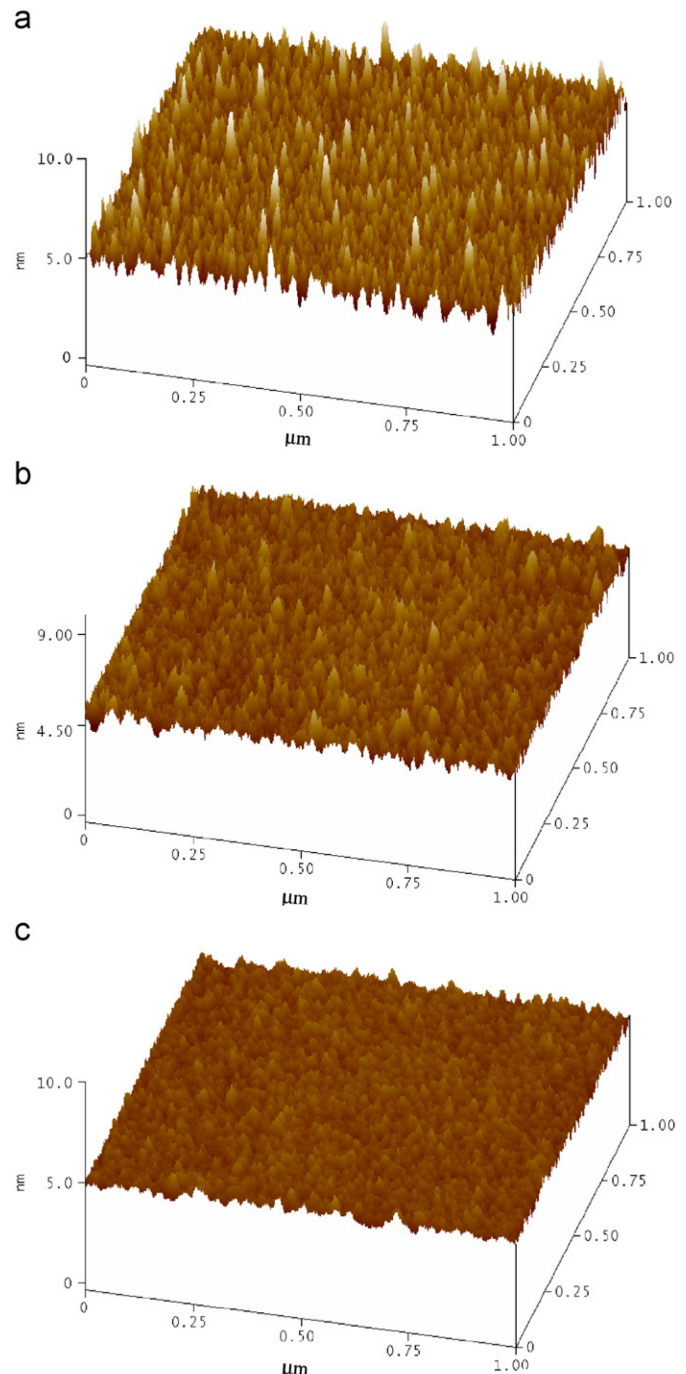

Fig. 4. AFM images of AlN buffers grown at temperature (a) 450 °C, (b) 740 °C and (c) 840 °C.

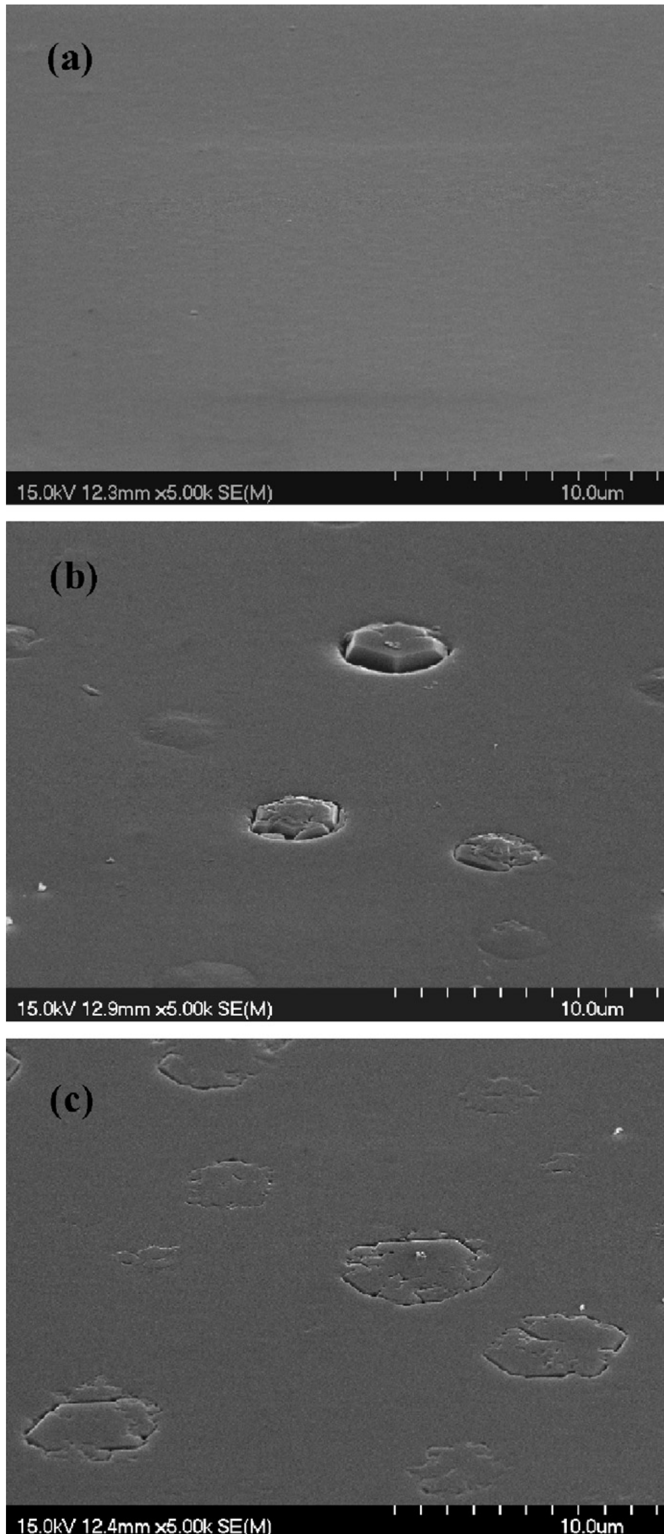

Fig. 5. SEM images of GaN surfaces grown on AlN buffer prepared at (a) 525 °C, (b) 485 °C and (c) 450 °C.

metal-organic chemical vapor deposition. The stress in the GaN film is, therefore, more difficult to relax when an AlN buffer is used.

A survey done by Pankove et al. [26] has shown that GaN grown on AlN buffer experienced larger stress than GaN grown on a GaN buffer. Therefore, a MBE-grown sample is always associated with larger stress than those grown using MOCVD. It is, thus, logical

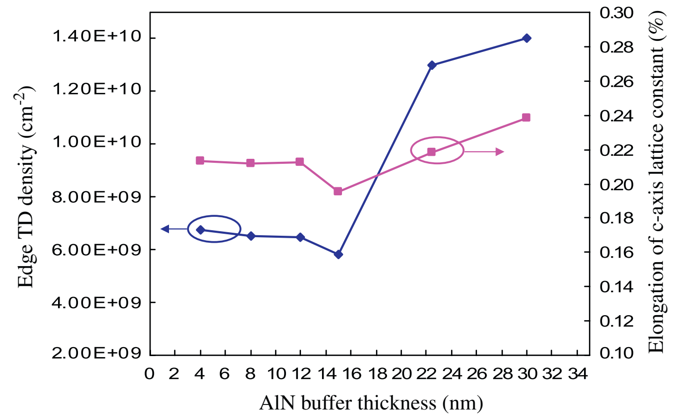

Fig. 6. The dependence of the XRD $(10\bar{1}2)$ FWHM and elongation of *c*-axis lattice constant on AlN buffer thickness.

that larger AlN thickness will induce larger stress values in the GaN [27]. Unexpectedly, however, larger stress is also encountered in GaN film grown on AlN thinner than 15 nm (Fig. 6). More studies should be conducted to understand the stress-relaxation mechanisms caused by the AlN buffer layer.

From all the above findings, we would now wish to discuss the effect of AlN growth parameters on the formation of edge TD and residual stress in GaN. For GaN grown on sapphire, the large stress generated should be relieved through the formation of misfit dislocation (at the materials interface) and/or plastic deformation in the crystal (achieved with dislocation glide). However, because the dislocations mobility in GaN is much less than with other III–V materials [28], the probability for them to glide in the crystal is low. Therefore, the edge TD density and its distribution were frozen in the GaN epilayer after growth and the lattice strain could not be relaxed through the plastic deformation [29]. In this case, the amount of edge TD could be used to trace the stress state in the GaN film (Fig. 3). Furthermore, since all the GaN films were grown at the same temperature, the amount of stress generated from thermal expansion difference was the same for all samples. So, the difference in residual stress of our GaN films should be a result of AlN surface roughness. The surface roughness of buffer layer might have induced the inclination of TDs in GaN [30], started from the AlN/GaN interface. The inclined TDs could promote the interaction of edge TDs, along the growth direction, and provided a misfit dislocation component that relieved the stress in GaN [30,31]. At the same time, the interaction of edge TDs with Burgers vectors of different signs could also enhance the recombination and annihilation [10,31] of TDs. Therefore, the reduction of stress and edge TD density in GaN were achieved with the formation of inclined TDs. On the other hand, however, for screw TDs, which all have Burgurs vectors with similar signs, recombination and annihilation of TD could not occur though interaction. Thus, the screw TD could only cluster together but their amount was not reduced as what we have seen.

4. Conclusions

We have investigated the effect of AlN buffer growth temperatures and thickness on the defect structure of GaN film. The buffer growth temperature was controlled but had contrary effects on screw and edge TDs densities. When grown on a lower-temperature AlN buffer with rougher surface, the edge and total TD densities in GaN were effectively reduced. This phenomenon can be explained by the formation of inclined TD that promoted the reduction of both stress and edge TD in GaN. Besides, this

stress was also affected by the buffer thickness. For the AlN buffer thinner or thicker than the optimum value, more stress and higher edge TD density were generated in GaN film. Thus, the edge TD density can be used as an indication of the stress state in GaN. On the other hand, the screw TD was increased with the use of lower-temperature AlN buffer (with rougher surface) but was not affected by the buffer thickness. In this study, GaN film grown on a 15-nm-thick buffer grown at 525 °C has a smooth surface (rms=0.56 nm) and relatively low total TD density ($5.8\times10^9\,cm^{-2}$). Smooth surface with low TD density are the two important factors for high-performance electronic device fabrication. Even though the dislocation density in GaN is still large as compared to other III–V materials, AlGaN/GaN structure HEMT device with good electrical performances has successfully been fabricated by Manfra et al. [2]. For comparison, their GaN material has TD density of about $5\times10^9\,cm^{-2}$ with surface roughness (rms) of 1 nm. In our study, the lowest TD density ($3.9\times10^9\,cm^{-2}$) GaN was grown on the 450 °C AlN buffer. But the surface of this GaN was less flat. However, we believe that this kind of surface can be recovered and smoothened with a thicker GaN film. Moreover, with a thicker film, the TD density can also be further reduced due to more interaction of the inclined TDs.

Acknowledgements

This work was financially supported by the Ministry of Economic Affairs and the National Science Council of Taiwan under the research grants of 95-EC-17-A-05-S1-020, NSC95-2752-E-009-001-PAE and NSC96-2221-E-009-236. The authors would like to thank ULVAC Taiwan Inc., and Micheal Chen, Chien-Ying Chen and Stanley Wu for the MBE maintenance support.

References

[1] A. Corrion, C. Poblenz, P. Waltereit, T. Palacios, S. Rajan, U.K. Mishra, J.S. Speck, IEICE Trans. Electron. E89-C (2006) 906.
[2] M.J. Manfra, N.G. Weimann, J.W.P. Hsu, L.N. Pfeiffer, K.W. West, S.N.G. Chu, Appl. Phys. Lett. 81 (2002) 1456.
[3] L.K. Li, B. Turk, W.I. Wang, S. Syed, D. Simonian, H.L. Stormer, Appl. Phys. Lett. 76 (2000) 742.
[4] O. Ambacher, J. Smart, J.R. Shealy, N.G. Weimann, K. Chu, M. Murphy, W.J. Schaff, L.F. Eastman, R. Dimitrov, L. Wittmer, M. Stutzmann, W. Rieger, J. Hilsenbeck, J. Appl. Phys. 85 (1998) 3222.
[5] M. Sumiya, S. Fuke, MRS Internet J. Nitride Semicond. Res. 9 (2004) 1.
[6] X.Q. Shen, H. Matsuhata, H. Okumura, Appl. Phys. Lett. 86 (2005) 021912.
[7] Y.B. Pan, Z.J. Yang, Z.T. Chen, Y. Lu, T.J. Yu, X.D. Hu, K. Xu, G.Y. Zhang, J. Crystal Growth 286 (2006) 255.
[8] E.J. Tarsa, B. Heying, X.H. Wu, P. Fini, S.P. DenBaars, J.S. Speck, Appl. Phys. Lett. 82 (1997) 5472.
[9] L. Zhou, D.J. Smith, D.F. Storm, D.S. Katzer, S.C. Binari, B.V. Shanabrook, Appl. Phys. Lett. 88 (2006) 011916.
[10] C.D. Lee, A. Sagar, R.M. Feenstra, C.K. Inoki, T.S. Kuan, W.L. Sarney, L. Salamance-Riba, Appl. Phys. Lett. 79 (2001) 3428.
[11] R.A. Oliver, M.J. Kappers, C.J. Humphreys, Appl. Phys. Lett. 89 (2006) 011914.
[12] T. Hino, S. Tomiya, T. Miyajima, K. Yanashima, S. Hashimoto, M. Ikeda, Appl. Phys. Lett. 76 (2000) 3421.
[13] J.C. Zhang, D.G. Zhao, J.F. Wang, Y.T. Wang, J. Chen, J.P. Liu, H. Yang, J. Crystal Growth 268 (2004) 24.
[14] D. Kapolnek, X.H. Wu, B. Heying, S. Keller, B.P. Keller, U.K. Mishra, S.P. DenBaars, J.S. Speck, Appl. Phys. Lett. 67 (1995) 1541.
[15] B. Shim, H. Okita, K. Jeganathan, M. Shimizu, H. Okumura, Jpn. J. Appl. Phys. 42 (2003) 2265.
[16] A.E. Romanov, P. Fini, J.S. Speck, J. Appl. Phys. 93 (2003) 106.
[17] X.Q. Shen, F. Kuruta, N. Nakamura, H. Matsuhata, M. Shimizu, H. Okumura, J. Crystal Growth 301–302 (2007) 404.
[18] C. Skierbiszewski, K. Dybko, W. Knap, M. Siekacz, W. Krupczyński, G. Nowak, M. Boćkowski, J. Łusakowski, Z.R. Wasilewski, D. Maude, T. Suski, S. Porowski, Appl. Phys. Lett. 86 (2005) 102106.
[19] M.J. Manfra, K.W. Baldwin, A.M. Sergent, R.J. Molnar, J. Caissie, Appl. Phys. Lett. 85 (2004) 1722.
[20] A.R. Smith, R.M. Feenstra, D.W. Greve, M.-S. Shin, M. Skowronski, J. Neugebauer, J.E. Northrup, Appl. Phys. Lett. 72 (1998) 2114.
[21] G. Koblmueller, R. Averbeck, L. Geelhaar, H. Riechert, W. Hösler, P. Pongratz, J. Appl. Phys. 93 (2003) 9591.
[22] B. Heying, X.H. Wu, S. Keller, Y. Li, D. Kapolnek, B.P. Keller, S.P. DenBaars, J.S. Speck, Appl. Phys. Lett. 68 (1995) 643.
[23] P. Gay, P.B. Hirsch, A. Kelly, Acta Metall. 1 (1953) 315.
[24] V.S. Harutyunyan, A.P. Aivazyan, E.R. Weber, Y. Kim, Y. Park, S.G. Subramanya, J. Phys. D: Appl. Phys. 34 (2001) A35.
[25] X.Q. Shen, M. Shimizu, H. Qkumura, Jpn. J. Appl. Lett. 42 (2003) L1293.
[26] A. Trampert, O. Brandt, K.H. Ploog, Crystal structure of group III nitrides, in: J.I. Pankove, T.D. Moustakas (Eds.), Gallium Nitride (GaN) I, Academic Press, New York, 1999, pp. 167–192.
[27] J. Keckes, G. Koblmueller, R. Averbeck, J. Crystal Growth 246 (2002) 73.
[28] L. Sugiura, J. Appl. Phys. 81 (1997) 1633.
[29] Y. Kim, S.G. Subramanya, H. Siegle, J. Krüger, P. Perlin, E.R. Weber, S. Ruvimov, Z. Liliental-Weber, J. Appl. Phys. 88 (2000) 6032.
[30] P. Cantu, F. Wu, P. Waltereit, S. Keller, A.E. Romanov, U.K. Mishra, S.P. DenBaars, J.S. Speck, Appl. Phys. Lett. 83 (2003) 674.
[31] P. Waltereit, C. Poblenz, S. Rajan, F. Wu, U.K. Mishra, J.S. Speck, Jpn. J. Appl. Phys. 43 (2004) L1520.